Influence of misfit dislocations on nanoisland decay

Carsten Sprodowski[1] and Karina Morgenstern[2,*]
[1]*Leibniz Universität Hannover, Institut für Festkörperphysik, Appelstrasse 2, D-30167 Hannover, Germany*
[2]*Ruhr-Universität Bochum, Lehrstuhl für physikalische Chemie I, Universitätsstrasse 150, D-44801 Bochum, Germany*

(Received 17 January 2019; revised manuscript received 29 May 2019; published 3 July 2019)

We investigate the decay of Ag islands on Cu(111) by variable low temperature scanning tunneling microscopy between 195 and 250 K. Such islands exhibit a misfit dislocation pattern forming (8×8) to (10×10) superstructures because of a major lattice mismatch between silver and copper. The decay of islands smaller than 200 nm^2 alternates between a slower and a faster decay. It is slower for specific island sizes, in particular those with magic numbers of superstructure unit cells. We relate these changes to the complexity of the heteroepitaxial decay, involving a deconstruction of the misfit dislocation pattern and a simultaneous diffusion of several adspecies during decay.

DOI: 10.1103/PhysRevB.100.045402

I. INTRODUCTION

The physical properties of nanoscale systems differ from those of macroscopic systems, making them attractive candidates to tune electronic or optical properties of matter, for instance, in quantum dots [1] or in three-dimensional (3D) nanoparticles [2]. However, nanostructures are thermodynamically only metastable. Even at room temperature, some alter their shape, and thus their properties in a short time interval [3,4]. In a coarsening process, referred to as Ostwald ripening, atoms diffuse from clusters with higher curvature to clusters with lower curvature, making smaller clusters shrink, while larger clusters grow at their expense. Only a profound understanding of the evolution of such nanoscale clusters in time will ultimately allow to produce stable ones in a controlled manner.

Consequently, the coarsening of nanostructures has been followed in real time in order to develop an atomic-scale understanding of Ostwald ripening, mainly employing low-energy electron microscopy (LEEM), e.g., [5–10], and scanning tunneling microscopy (STM) [3,4]. LEEM studies focused on high-temperature changes on high-melting materials as Rh(001) [11], Si(110) [12], W(100) [13], or quasicrystals [14]; STM research studied decay at or around room temperature on Cu and Ag surfaces [3,4,15,16]. Both techniques concentrated for 20 years on homoepitaxial nanostructures of monatomic height, which are named adatom islands. More recently, heteroepitaxial bimetallic systems moved into the focus of attention [13,17–21]. A difference in lattice constants between deposit and substrate tends to lead to overlayers of unique structure in heteroepitaxy [22]. The influence of such structures on Ostwald ripening remains to be explored.

The lattice mismatch between the here investigated Ag(111) and Cu(111) surfaces is, at 13%, substantial [23,24]. The Ag/Cu(111) system has thus been intensely investigated as a representative for a large deposit on a substrate with small lattice constant. Despite the large mismatch, the Ag superstructures are only slightly compressed with respect to the Ag bulk values [25]. Early room temperature studies identified a dislocation network by high energy electron diffraction [26] and a $p(9 \times 9)$ superstructure by low energy electron diffraction (LEED) [27]. However, $p(8 \times 8)$, $p(9 \times 9)$, and $p(10 \times 10)$ superstructures are similar in energy [25], consistent with STM studies [28–30]. These closely related coincidence structures coexist. They consist of differently sized partial dislocation loops in the topmost Cu layer altering the adsorption sites of the Ag overlayer atoms in a favorite manner. The loops result from a restructuring of the Cu surface, for which some Cu atoms are removed and others are shifted from fcc to hpc sites [cf. Fig. 1(g)]. In this way, Ag atoms avoid energetically unfavorable on-top adsorption sites that would be part of a simple moiré pattern [31]. The dislocation loops force one distinct orientation of the coincidence lattice with the substrate lattice, in contrast to the flexible angles possible for moiré superstructures.

In this article, we investigate the decay of Ag islands on Cu(111) by fast scanning tunneling microscopy. Distinct island sizes have increased stability, slowing down the overall decay. Changes between these distinct island sizes and the final decay are much faster. We relate these more stable sizes to the misfit dislocations and thus to the lattice mismatch. The dislocation network forces slow decay only for specific island sizes, in particular for magic numbers of superstructure units. The magic number, at which this final decay sets in, is temperature dependent.

II. EXPERIMENTAL METHODS

STM measurements are performed with a fast scanning STM under ultra-high vacuum (UHV) conditions (base pressure 2×10^{-10} mbar). The Cu(111) sample is prepared by cycles of Ar^+ sputtering (1.3 keV, 3 to 5×10^{-5} mbar, 8 to 15μA, 10 to 30 min) and annealing up to 970 K (10 to 45 min). Ag is deposited from a resistively heated Ag wire, which is attached to a tungsten filament for this purpose. The

*karina.morgenstern@rub.de

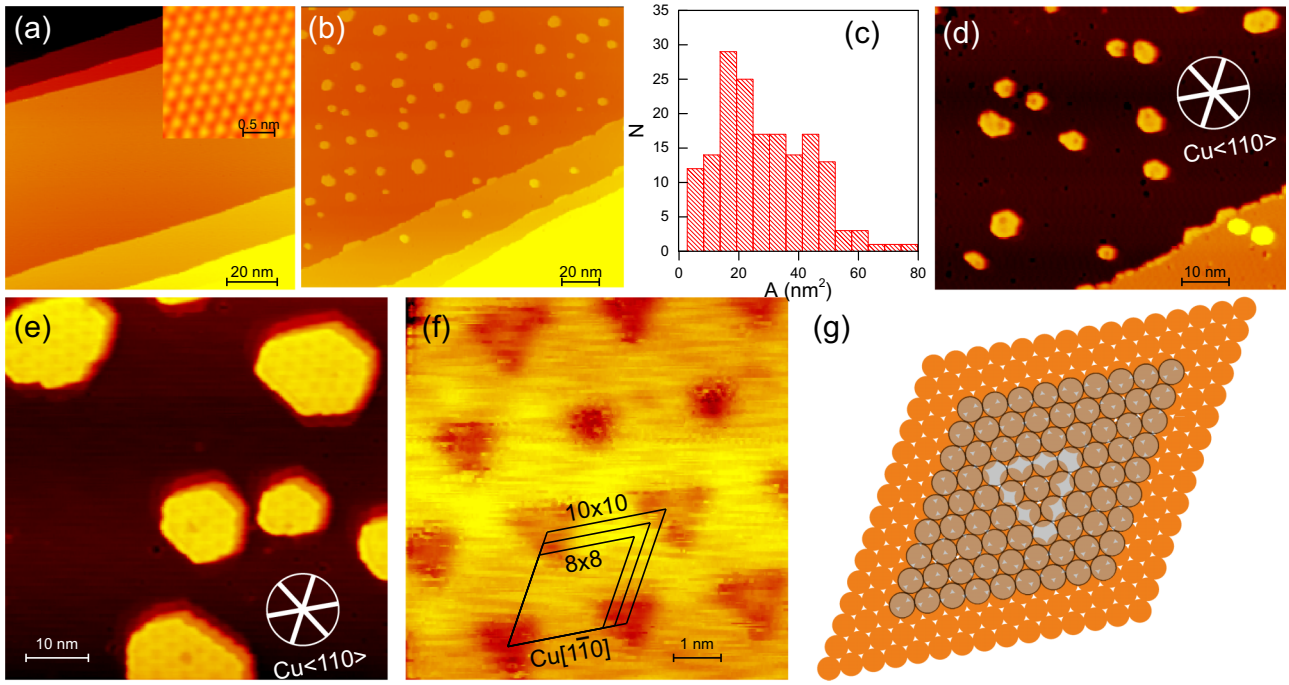

FIG. 1. Surface preparation: (a) Pristine Cu(111) surface after cleaning procedure, 0.36 nA, 994 mV; inset: Atomic resolution with one Gaussian smooth. (b) Overview image after sputter-aided deposition of 0.1 ML Ag, 0.36 nA, 857 mV. (c) Statistics of island sizes. (d),(e) Detail images after sputter-aided deposition; coverage in (e) 2.5 times the coverage of (d), cross marks high symmetry Cu directions derived from the inset in (a). (d) 0.39 nA, 857 mV (e) 0.41 nA, 831 mV. (f) Zoom to top of an islands as in (e), (*nxn*) unit cells are marked, 18 nA, 625 mV. (g) Structural model of (9 × 9) superstructure unit cell with dislocation loop in Cu layer; Cu atoms in orange, Ag atoms in semitransparent gray [28].

surface is held between 200 K and room temperature during deposition. The rate is between 10^{-3} and 0.5 ML/min. During metal deposition the pressure stays below 3×10^{-10} mbar.

The natural island density is so small that Ag islands nucleate almost exclusively at the step edges, even at the lowest deposition temperature at which a dislocation network forms. We artificially enhance this density for the decay studies by giving a 1s Ar^+ sputter pulse (0.4 to 0.7 keV, 1×10^{-6} mbar) directly before deposition. Such a short sputter pulse leads to small atom clusters around each ion impact [32]. The few Cu atoms produced in this way serve as nuclei for island growth [33]. After such a sputter-aided deposition, the island density is considerably enhanced (see [34]). The clusters and vacancies created, which do not serve as nuclei, anneal on the timescale of seconds, long before the decay measurements are started [32]. Thus, the terraces beyond the islands are defect free during the decay measurements, as confirmed by STM. Seldomly, a small defect remains for some images at the end of an island decay (cf. island 3 in Fig. 5). Such a defect in not expected to influence the decay of the island at much larger island size.

The island decay is monitored by scanning the same region of the surface repeatedly for some hours. As the STM is lacking active cooling, there is a small increase in temperature during these measurements, up to 5 K per hour. For the quantitative determination of decay exponents data, we use only data, for which the temperature change is less than 1 K.

III. RESULTS AND DISCUSSION

The pristine Cu(111) surface consists of large terraces separated by step bundles [Fig. 1(a)]. The orientation of the surface lattice, inferred from images with atomic resolution [Fig. 1(a), inset], is identical throughout the here presented experiments. After sputter-aided deposition, islands are randomly distributed over the surface [Fig. 1(b)] with a size distribution typical for metal-on-metal growth [Fig. 1(c)]. The islands are mainly hexagonal with straight steps along the Cu⟨110⟩ surface directions [Fig. 1(d)].

Higher z-resolution reveals a superstructure on the islands [Fig. 1(d)]. This superstructure is better visible for larger islands, grown under the same conditions [Fig. 1(e)]. The top of such an island is covered by well-separated triangular structures of smaller apparent height than the rest of the island, here forming a (10 × 10) unit cell [Fig. 1(f)], in line with the (8 × 8) to (10 × 10) superstructures grown without a sputter pulse at somewhat higher temperature before [25]. The observed triangles correspond to the misfit dislocation loops discussed in the introduction [Fig. 1(g)]. For the (9 × 9) superstructure, four Cu atoms are removed from the surface plane and a triangle of six Cu atoms is displaced from fcc to hcp sites [middle of Fig. 1(g)]. The Ag atoms adsorbed above these dislocation lines are adsorbed at a lower distance to the surface plane giving rise to the reduced height in STM images [Fig. 1(f)]. It is the Ag atom right above the middle of the displaced triangle that profits most from the surface

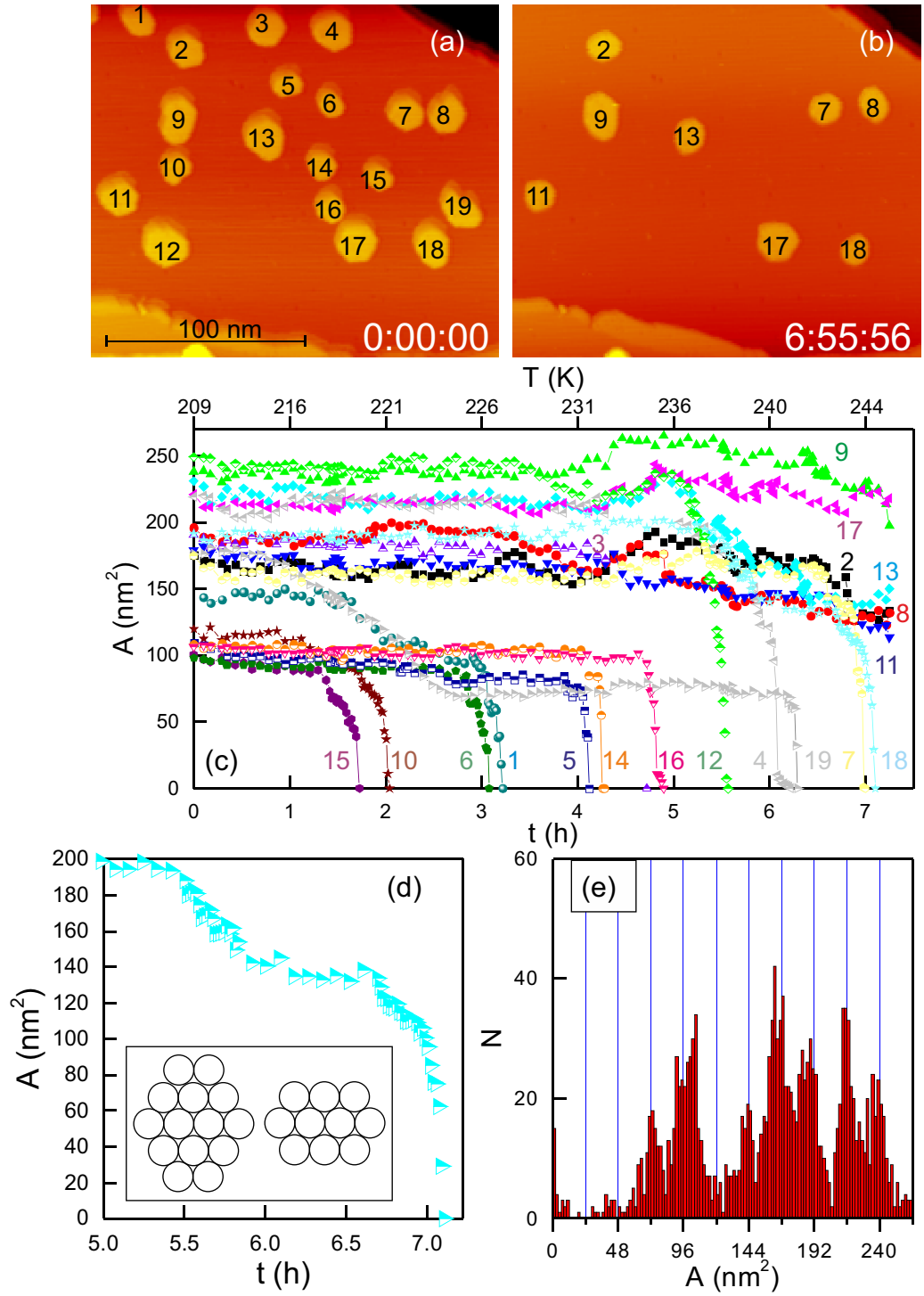

FIG. 2. Decay of Ag islands on Cu(111) at (225 ± 15) K after 1 s sputter pulse at 178 K and deposition for 79 s at (194 ± 16) K: (a),(b) STM images at beginning and at end of movie; 340 pA, −884 mV. (c) Area A of marked islands in time t. (d) Last hours of decay of island 18; inset shows magic cluster sizes (see text). (e) Histogram of all area values from (c).

reconstruction as it would be adsorbed in an energetically unfavorable on-top site without the reconstruction and now resides in a hollow site [Fig. 1(g)]. Note that the smaller islands in Figs. 1(b) and 1(d) are likewise reconstructed by dislocation loops, as are all islands investigated in this article. The reconstruction is not visible at the resolution employed during the decay experiments.

Having clarified the structure of the islands, we now follow the decay of such smaller islands by repeatedly imaging the same spot of the surface. In the example shown in Figs. 2(a) to 2(b), around half of the islands decay within seven hours. Their decay curves differ considerably from decay curves of isolated islands in homoepitaxial systems, for which decay rates change continuously, if they change [4].

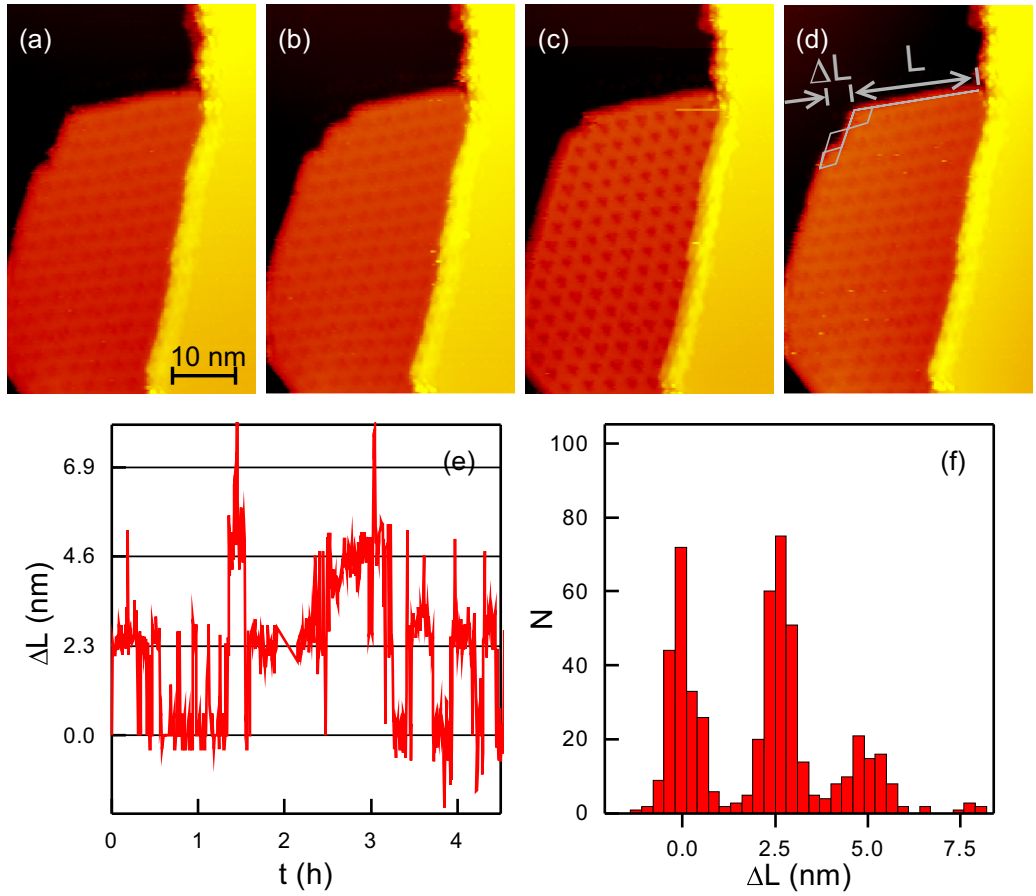

FIG. 3. Island shape fluctuation at room temperature: (a)–(d) Snapshot of movie of a Ag island at a Cu(111) step edge; contour of the upper border of the four images drawn in (d); 418 images at $\Delta t = 20$ s; deposition: 6 min at room temperature, 530 pA, 1.2 V. (e) Length of upper edge ΔL with respect to length in first image; for a definition see (d). (f) Histogram of length changes from (e).

To understand this difference, we shortly recapitulate the quasi-equilibrium theory used to describe decay in homoepitaxial systems. In the model, the area A of an island decays monotonously with either the same rate or a steadily increasing rate. This was described theoretically through application of the classical theory of cluster ripening [developed by Lifshitz, Sloyozov, and Wagner (LSW)] to surfaces by Chakraverty, Wynblatt, and Gjostein [35,36]. In this description, a circular adatom island with radius r is surrounded by a circular step with radius R. The latter acts as a sink for the adatoms. Integration of the stationary diffusion equation for the flux between these borders leads to a power law for the time evolution of the island's radius $r(t)$ [4]:

$$r(t)^2 \propto A(t) \propto \tau^{2\beta} \text{ with } \tau = (t_0 - t) \qquad (1)$$

for an island that is completely decayed at t_0. The exponent β reflects the rate limiting step. If the diffusion of adatoms between the two borders is rate limiting, then $\beta = 1/3$ and the decay is called diffusion-limited, e.g., observed for Ag/Ag(111) [37] and for Si/Si(111) [9,10]. The experimental value $\beta = 0.27 \pm 0.06$ in the former case deviates from the calculated value $\beta = 1/3$. This deviation is expected at small island sizes for which linearization of an exponential term, used for the derivation, leads to inaccuracies. The exponent of $\beta = 1/2$, corresponding to a linear decay in time, reflects an interface-limited decay. Interface-limited decay is only rarely observed in homoepitaxial systems [38], but, for instance, for hut-shaped Cu structures on W(100) [13]. This quasi-equilibrium model is strictly valid only for islands that adapt an equilibrium shape that can be described by a single curvature. Thus, islands consisting of only a few ten atoms or faceted islands are ill-described. The islands, we investigate here are in the range or larger than those described successfully before [4]. Note, however, that the larger islands here are rather hexagonal than circular [Fig. 1(d)]. Thus, describing the adatom density based on the real radius introduces quantitative errors. For a correct description, an apparent radius, describing the adatoms density in front of the faceted island's edge correctly, should be used instead. Independent of this quantitative inaccuracy, the distinct qualitative change between different decay rates is not explainable by this model.

Abrupt changes between different decay rates, as observed in Fig. 2(c), have been observed for stacks of islands, when the top-most decaying island approaches the descending edge [39,40]. In this case, the detachment rate from the island is altered by the close proximity of the island to another step edge. This suggests that the abrupt changes in decay observed

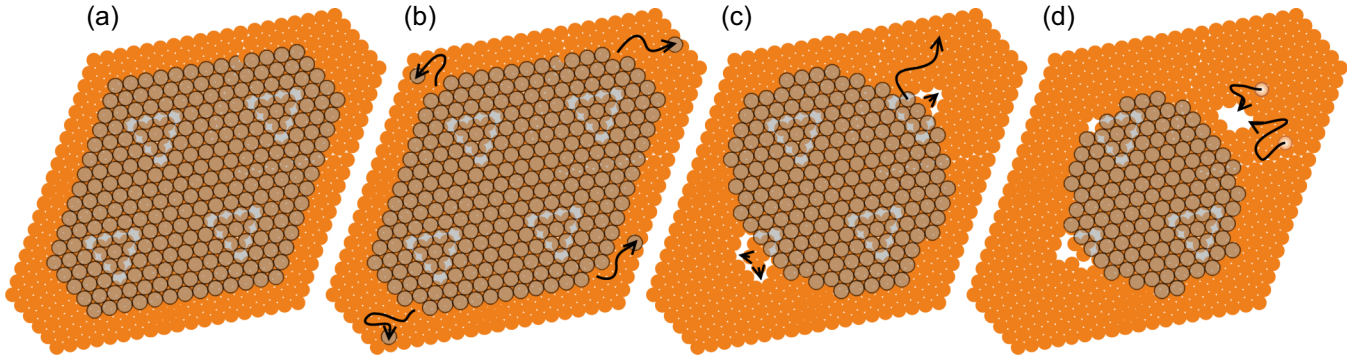

FIG. 4. Scheme of processes involved in the decay of a dislocation reconstructed island; Cu atoms in orange; bold in surface layer; with shade in adsorbate layer; Ag atoms in half-transparent gray: (a) island with four dislocation loops, (b) detachment of Ag atoms far away from dislocation loops, (c) detachment of Ag atoms at dislocation loops and motion of Cu within surface layer from hcp to fcc sites, (d) filling of vacancy island by diffusing Cu atoms.

here are related to differences in detachment barrier from the islands during different stages of the decay.

For identifying reasons for this variation in detachment barrier, we analyze the decay curves quantitatively. The Ag islands on Cu(111) of our study mostly decay linearly at a small rate below 6×10^{-4} nm^2/s [Fig. 2(c)]. Islands larger than 150 nm^2 grow at similar rates. Sometimes also islands in the size range between 150 and 100 nm^2 grow, if a smaller island decays in close proximity, reflecting the local nature of Ostwald ripening [41].

The decay of the islands accelerates sharply, if islands get smaller than approx. 70 nm^2, to a rate of 0.01 to 0.1 nm^2/s. This fast decay is sometimes slowed again at around 55 nm^2, before the island disappears completely, e.g., island 15 in Fig. 2(c). This alternation between more rapid decays and slower decays also operates at larger islands sizes, as exemplified for island 18 in Fig. 2(d).

Remarkably, the more stable island sizes are largely temperature independent. A statistics of all sizes measured within the temperature range of 35 K of the movie in Figs. 2(a) to 2(b) reveals that multiples of 18 nm^2 are clearly preferred [Fig. 2(e)] [42]. The smallest stable sizes in Fig. 2(e) are $n = 3$ and $n = 4$, corresponding to 54 and 72 nm^2, respectively, approximately 10 or 14 unit cells of a (9×9) superstructure. Smaller multiples of superstructure unit cells are stable at lower temperature (cf. Fig. 6). Note that for heteroepitaxial diffusion of Cu islands on Ag(111) magic island sizes up to 15 atoms were reported [43,44]. In this case, dislocations in the Cu islands allow a faster diffusion, which is more likely for specific island shapes. These islands are much smaller than our islands and thus the reason for their behavior cannot be explained by a dislocation motion.

The coincidence between multiples of the superstructure unit cells and stable island sizes suggests that the dislocation pattern stabilizes certain island sizes. Moreover 10 and 14 unit cells can be considered as magic numbers as they lead to clusters of high symmetry with side lengths of either two or three [see Fig. 2(d), inset]. Unfortunately, it is not possible to image the superstructure on the smaller islands during decay without disturbing them by the scanning process. However, our interpretation of superstructure unit cells stabilizing island sizes is corroborated by fluctuations at the border of larger islands grown without a sputter pulse at room temperature [Figs. 3(a) to 3(d)]. The border of such larger islands is mostly faceted along the unit cells of the dislocation network. In time, the island border fluctuates, and specific segments dis- and reappear [cf. contour in Fig. 3(d)]. The impression of a collective disappearance and reappearance of segments is corroborated by the length changes of the upper edge [Fig. 3(e)]. The length changes preferentially by either 2.1 nm or by 4.2 nm [Fig. 3(f)]. The values correspond to approximately $n \cdot 8 \cdot a_{Cu} = 2.04$ nm, in line with the (8×8) superstructure observed here.

In homoepitaxial decay only two processes are involved, detachment of atoms from the island and self-diffusion of adatoms over the terrace. In contrast, there are more processes involved in the Ag/Cu(111) system, depicted in Fig. 4. Because of the dislocation lines, different atoms have different binding heights leading to different detachment barriers. Atoms far away from the dislocation triangles will not be influenced by them and may detach and diffuse with only the two processes relevant as in the homoepitaxial case [Fig. 4(b)]. It is generally accepted that such a detachment leads to diffusion-limited decay [4]. However, certainly above the dislocation lines and possibly close to them, Ag atoms are more strongly bound, leading to an increased barrier for adatom detachment [Fig. 4(c)]. In addition, the Cu surface needs to rearrange to eventually lead to the flat surface observed in the experiment after complete decay. This demands a motion of the Cu adatoms from hcp to fcc sites [Fig. 4(c)] leading to vacancy clusters. The filling of the vacancy islands is another barrier for decay. Additional barriers at one of the interfaces result in an interface-limited decay [4]. Though fitting of Eq. (1) to the segments of slow decay does not converge in a single minimum because of the three fitting parameters involved, $\beta > 0.5$ is mostly obtained, corroborating our interpretation. It is further corroborated by the insensitivity of neighboring islands from their direct environment, unless there is a fast decay in their vicinity. Whether the slow decay is limited by the detachment of the Ag atoms from the dislocation lines or by the filling of the vacancies created by dislocation relieve cannot be solved by experiments alone.

The remaining vacancy clusters could either be removed by vacancy cluster motion to eventually be filled at Cu step edges

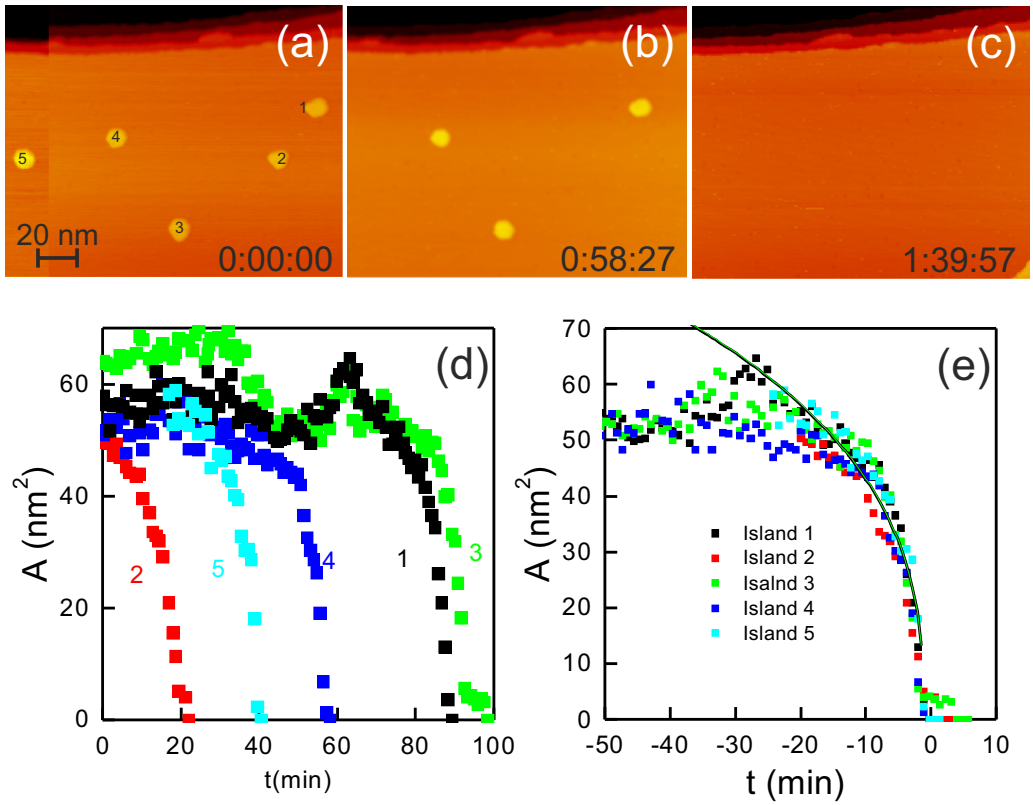

FIG. 5. Final decay of an ensemble of Ag islands of similar size on Cu(111) at (215 ± 10) K; produced by sputter pulse at 185 K and deposition for 48 s at (191 ± 7) K. (a)–(c) STM images at beginning, middle, and end of movie, respectively; t in h:min:s, 335 pA, −884 mV (d) area evolution in time (e) time shifted area evolution of (d) to common point of final decay $t_0 \approx 0$ with fit of $A(t_0 - t)^{2\beta}$ yielding $2\beta = 0.355$.

or they might be filled by diffusing Cu adatoms [Fig. 4(d)]. The islands that grow are the natural source of these Cu adatoms, as during formation of new dislocation lines Cu adatoms are expelled from the surface. This suggests that there are both Ag and Cu adatoms diffusing simultaneously during decay. The diffusion energy of Ag atoms on Cu(111) has been calculated recently as 23 meV [45]. It is thus of the same order and only slightly smaller than the self-diffusion energy of Cu/Cu(111), at 28 meV [46]. Consequently, both atomic species should be able to diffuse between decaying and growing islands on the same time scale. Despite both atoms present, there is no indication of alloy formation, neither in the terrace nor at the growing island. This observation is in agreement with earlier measurements at somewhat higher temperature, where alloy formation was only observed on vicinal surfaces [30]. The likely reason is the large difference in size and thus lattice constant between the two species.

As soon as a dislocation triangle and the attached Ag adatoms are completely removed, a large number of atoms can be released quickly; those that are not adsorbed in the close vicinity of the neighboring dislocation triangles. The segments of fast decay are too short to determine 2β. According to our model, only Ag atoms detach in this case and no other processes are involved. This implies that the decay is diffusion-limited, as discussed above. This interpretation is corroborated by the final fast decay of islands smaller than 54 nm^2, one of the "magic" island sizes. All of the small island in the ensemble in Figs. 5(a) and 5(b) show the same behavior within the last 10 min [Fig. 5(c)], best seen by shifting the time axis to a common $t_0 \approx 0$ [Fig. 5(d)]. This decay is clearly nonlinear, increasing in rate with smaller island sizes. This is the typical behavior for diffusion-limited decay, because the decay rate for small islands should increase at decreasing island size for interface-limited decay [4]. Note that the islands in Fig. 5 are rather circular such that the theory discussed above is more applicable than for the larger islands. Fitting Eq. (1) to the last 10 min of decay yields an exponent of $2\beta = 0.355$ [Fig. 5(d)]. For islands of these sizes, at some 10 nm^2, the theory has been successfully applied for the decay of Ag islands on Ag(111) [37]. This value is smaller than the one derived for diffusion-limited decay in the homoepitaxial case. The simple theory thus should be adapted to the heteroepitaxial case. We tentatively propose that the strain induced by the lattice mismatch leads to a variation in binding energy of the Ag atoms for these small islands and thus to an adatom density that is not strictly proportional to the island's curvature. The exponent is, however, a robust value for the here investigated system, Ag/Cu(111). 2β does not depend on temperature within the investigated temperature range between 194 an 252 K. The mean for all investigated islands is $2\beta = 0.364 \pm 0.141$.

The temperature dependence of the decay is demonstrated in Fig. 6(a). In the temperature range between 217 and 257 K,

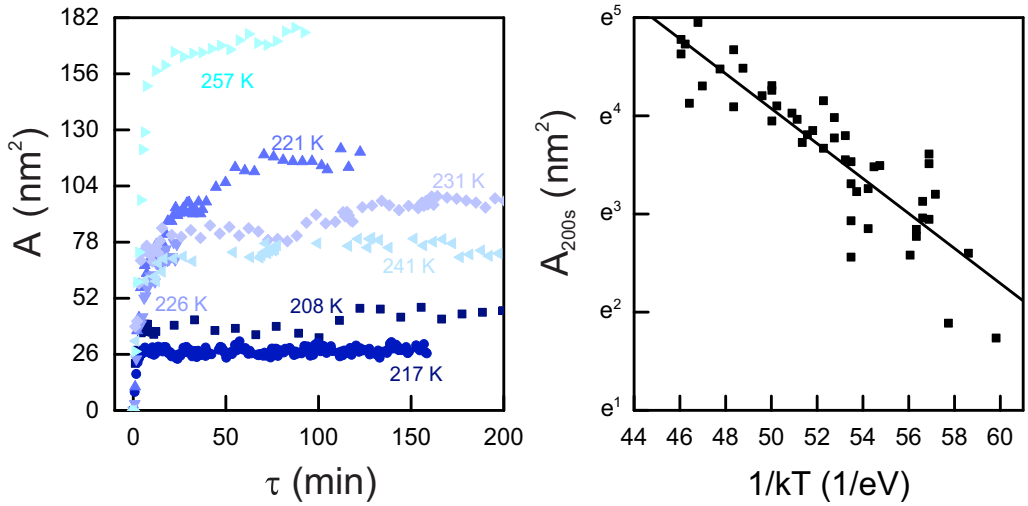

FIG. 6. Temperature dependence of final decay: (a) final decay at different indicated temperatures: Area A vs. decay time τ (b) Arrhenius plot of island size at 200 s before final decay A_{200s}; fit yields slope of (0.18 ± 0.01) eV.

the final decay takes the longer, the lower the temperature is, as expected for an activated process. Moreover, the smallest stable island size is temperature dependent being only 26 nm^2 for the lowest and more than 160 nm^2 for the highest temperature. To quantify this observation, we fitted the final decay of all investigated islands by Eq. (1) to determine the size of each island at 200 s before its complete decay more precisely than given by our discrete data points. The time value is chosen, because this is the largest value, at which all islands are already in the diffusion-limited decay regime. Thus, the energies involved in this process are not related to the increased barrier induced by the dislocation network. Only in this regime it is justified to use the simple theory of Eq. (1) developed for homoepitaxial systems.

In the investigated temperature range between 194 and 252 K, the data fall on a straight line in an Arrhenius plot [Fig. 6(b)]. Note that the scatter in the data results partly from different environments of the decaying islands as neighboring islands influence the local adatom density, partly from the three fitting parameters in Eq. (1), which allow equally good fits for some variation in t_0. The scatter does, however, not impede to determine an activation energy of (0.178 ± 0.01) eV from fitting a straight line in the Arrhenius plot. Due to the other uncertainties, the error bar of the fit is certainly not the error bar of the energy determined. The activation energy corresponds to the activation energy for island decay in the diffusion-limited regime. It is thus a combination of the diffusion energy of Ag on Cu(111) and the detachment energy for Ag from Ag islands on Cu(111). The diffusion energy of Ag atoms on Cu(111) has been calculated recently as 23 meV [45]. This implies that the detachment energy of a Ag atom from a Ag island on Cu(111) during final decay is, on average, $\approx$0.155 eV. This barrier is considerably lower than expected. A possible explanation for such a low barrier could be impurities, as trace amounts of chalcogenes were shown to increase kintetics considerably [47–49]. However, our mass spectra of the base pressure do not show any indication for oxygen or sulfur. Further explanation could be the strain release in smaller islands due to the lattice mismatch between the material. We hope to induce theoretical work with this report to understand this unusually low activation energy.

The existing models are too simple to describe the whole decay, including the interface-limited parts. As the decay in interface-limited decay is orders of magnitudes slower, the detachment energy of magic islands must be much larger. In fact, the activation energy for mound decay of Ag islands on Cu(111) is, at (1.0 ± 0.1) eV for thick and (0.70 ± 0.15) eV for thinner mounds, much larger [24]. As in these kind of studies rate-limiting steps determine the overall decay, which, to our study, is interface-limited and slow, the barrier determined in [24] should be the upper limit of the interface-limited decay of the monatomic islands investigated here, which, as expected, has a considerably higher barrier than the one determined for diffusion-limited decay.

IV. CONCLUSION

In conclusion, the detachment of atoms from Ag islands on Cu(111) is strongly influenced by their misfit dislocation network. This network stabilizes specific sizes of the islands, in particular, if the island has a size close to magic multiples of superstructure unit cells. Between these sizes the island decays rapidly due to a smaller detachment barrier and no need for removal of dislocation lines. The stabilization of certain island sizes should likewise hold for other dislocation networks, i.e., Au/Ni(111), and other systems with a large lattice mismatch. It can lead to island ensembles of rather uniform size, e.g., Fig. 5, which is not expected from ripening scenarios usually described and observed in homoepitaxy.

ACKNOWLEDGMENTS

This work was supported by the Research Training group "Confinement-controlled Chemistry," which is funded by the Deutsche Forschungsgemeinschaft (DFG) Grant No. GRK2376/331085229.

[1] S. M. Reimann and M. Manninen, Rev. Mod. Phys. **74**, 1283 (2002).
[2] M. Pelton, J. Aizpurua, and G. Bryant, Laser Photonics Rev. **2**, 136 (2008).
[3] M. Giesen, Prog. Surf. Sci. **68**, 1 (2001).
[4] K. Morgenstern, Phys. Status Solidi B **242**, 773 (2005).
[5] W. Theis, N. C. Bartelt, and R. M. Tromp, Phys. Rev. Lett. **75**, 3328 (1995).
[6] N. C. Bartelt, W. Theis, and R. M. Tromp, Phys. Rev. B **54**, 11741 (1996).
[7] H. Hibino, C.-W. Hu, T. Ogino, and I. S. T. Tsong, Phys. Rev. B **63**, 245402 (2001); Ostwald ripening of two-dimensional islands on Si(001).
[8] H. Hibino, Y. Watanabe, C.-W. Hu, and I. S. T. Tsong, Phys. Rev. B **72**, 245424 (2005).
[9] K. L. Man, A. B. Pang, and M. S. Altman, Surf. Sci. **601**, 4669 (2007).
[10] A. B. Pang, K. L. Man, M. S. Altman, T. J. Stasevich, F. Szalma, and T. L. Einstein, Phys. Rev. B **77**, 115424 (2008).
[11] G. L. Kellogg and N. C. Bartelt, Surf. Sci. **577**, 151 (2005).
[12] F. Watanabe, S. Kodambaka, W. Swiech, J. E. Greene, and D. G. Cahill, Surf. Sci. **572**, 425 (2004).
[13] T. R. J. Bollmann, R. van Gastel, H. Wormeester, H. J. W. Zandvliet, and B. Poelsema, Phys. Rev. B **85**, 125417 (2012).
[14] S. Förster, J. I. Flege, E. M. Zollner, F. O. Schumann, R. Hammer, A. Bayat, K.-M. Schindler, J. Falta, and W. Widdra, Ann. Phys. (N.Y.) **529**, 1600250 (2017).
[15] P. A. Thiel, M. Shen, D.-J. Liu, and J. W. Evans, J. Phys. Chem. C **113**, 5047 (2009).
[16] Y. Han, S. M. Russell, A. R. Layson, H. Walen, C. D. Yuen, P. A. Thiel, and J. W. Evans, Phys. Rev. B **87**, 155420 (2013).
[17] C. T. Campbell, S. C. Parker, and D. E. Starr, Science **298**, 811 (2002).
[18] Y. Han, B. Unal, F. Qin, D. Jing, C. J. Jenks, D.-J. Liu, P. A. Thiel, and J. W. Evans, Phys. Rev. Lett. **100**, 116105 (2008).
[19] C. Zaum, M. Rieger, K. Reuter, and K. Morgenstern, Phys. Rev. Lett. **107**, 046101 (2011).
[20] C. Zaum, J. Meyer, K. Reuter, and K. Morgenstern, Phys. Rev. B **90**, 165418 (2014).
[21] A. Beichert, C. Zaum, and K. Morgenstern, Phys. Rev. B **92**, 045422 (2015).
[22] J. Jacobsen, L. P. Nielsen, F. Besenbacher, I. Stensgaard, E. Lægsgaard, T. Rasmussen, K. W. Jacobsen, and J. K. Nørskov, Phys. Rev. Lett. **75**, 489 (1995).
[23] $a_{\mathrm{Ag}} = 0.289\,\mathrm{nm}$, $a_{\mathrm{Cu}} = 0.255\,\mathrm{nm}$.
[24] U. Kürpick, G. Meister, and A. Goldmann, Appl. Surf. Sci. **89**, 383 (1995).
[25] S. M. Foiles, Surf. Sci. **292**, 5 (1993).
[26] E. Bauer, Z. Kristallogr. **110**, 372 (1958).
[27] E. Bauer, Surf. Sci. **7**, 351 (1967).
[28] I. Meunier, G. Tréglia, J.-M. Gay, B. Aufray, and B. Legrand, Phys. Rev. B **59**, 10910 (1999).
[29] R. Tetot, F. Berthier, J. Creuze, I. Meunier, G. Treglia, and B. Legrand, Phys. Rev. Lett. **91**, 176103 (2003).
[30] D. O. Bellisario, J. W. Han, H. L. Tierney, A. E. Baber, D. S. Sholl, and E. C. H. Sykes, J. Phys. Chem. C **113**, 12863 (2009).
[31] W. E. McMahon, E. S. Hirschhorn, and T.-C. Chiang, Surf. Sci. Lett. **279**, L231 (1992).
[32] C. Sprodowski and K. Morgenstern, Phys. Rev. B **82**, 165444 (2010).
[33] G. Rosenfeld, N. N. Lipkin, W. Wulfhekel, J. Kliewer, K. Morgenstern, B. Poelsema, and G. Comsa, Appl. Phys. A **61**, 455 (1995).
[34] See Supplemental Material at http://link.aps.org/supplemental/10.1103/PhysRevB.100.045402 for further details about the preparation of the investigated island ensembles via sputter-aided deposition.
[35] B. K. Chakraverty, J. Phys. Chem. Solids **28**, 2401 (1967).
[36] P. Wynblatt and N. A. Gjostein, Prog. Solid State Chem. **9**, 21 (1975).
[37] K. Morgenstern, G. Rosenfeld, and G. Comsa, Phys. Rev. Lett. **76**, 2113 (1996).
[38] K. Morgenstern, G. Rosenfeld, E. Lægsgaard, F. Besenbacher, and G. Comsa, Phys. Rev. Lett. **80**, 556 (1998).
[39] K. Morgenstern, G. Rosenfeld, G. Comsa, E. Lægsgaard, and F. Besenbacher, Phys. Rev. Lett. **85**, 468 (2000).
[40] K. Morgenstern, G. Rosenfeld, G. Comsa, M. R. Sørensen, B. Hammer, E. Lægsgaard, and F. Besenbacher, Phys. Rev. B **63**, 045412 (2001).
[41] K. Morgenstern, G. Rosenfeld, and C. Comsa, Surf. Sci. **441**, 289 (1999).
[42] Note that in this particular example $n = 1, 2, 5$ do not exist and $n = 3, 6$ are less frequently observed, but not in general.
[43] A. W. Signor, H. H. Wu, and D. R. Trinkle, Surf. Sci. **604**, L67 (2010).
[44] H. H. Wu, A. W. Signor, and D. R. Trinkle, J. Appl. Phys. **108**, 023521 (2010).
[45] A. Kotri, E. El koraychy, M. Mazroui, and Y. Boughaleb, Surf. Interface Anal. **49**, 705 (2017).
[46] M. Karimi, T. Tomkowski, G. Vidali, and O. Biham, Phys. Rev. B **52**, 5364 (1995).
[47] W. L. Ling, N. C. Bartelt, K. Pohl, J. dela Figuera, R. Q. Hwang, and K. F. McCarty, Phys. Rev. Lett. **93**, 166101 (2004).
[48] J. Kibsgaard, K. Morgenstern, E. Lægsgaard, J. V. Lauritsen, and F. Besenbacher, Phys. Rev. Lett. **100**, 116104 (2008).
[49] P. A. Thiel, M. Shen, D.-J. Liu, and J. W. Evans, J. Vac. Sci. Technol. A **28**, 1285 (2010).